A cocktail of 165 Er(iii) and Gd(iii) complexes for quantitative detection of zinc using SPECT and MRI

Kyangwi Malikidogo, Isidro da Silva, Jean-François Morfin, Sara Lacerda, Laurent Barantin, Thierry Sauvage, Julien Sobilo, Stéphanie Lerondel, Éva Tóth, Célia Bonnet

Journal Name

COMMUNICATION

A cocktail of ^{165}Er(III) and Gd(III) complexes for quantitative detection of zinc by SPECT and MRI

Received 00th January 20xx,
Accepted 00th January 20xx

DOI: 10.1039/x0xx00000x

www.rsc.org/

Patrick K. Malikidogo,[a] Isidro Da Silva,[b] Jean-François Morfin,[a] Sara Lacerda,[a] Laurent Barantin,[c] Thierry Sauvage,[b] Julien Sobilo,[d] Stéphanie Lerondel,[d] Éva Tóth*[a] and Célia S. Bonnet*[a]

We propose quantitative assessment of zinc by combining nuclear and MR imaging. We use a cocktail of a Gd^{3+}-complex providing a Zn^{2+}-dependent MRI response, and its $^{165}Er^{3+}$ analogue allowing for concentration assessment. ^{165}Er is readily obtained in a cyclotron and purified, which is indispensable for successful quantification of metal ions.

Molecular imaging seeks to characterize the physical-chemical state of tissues such as pH, the presence of enzymes, metabolites or ions. Magnetic Resonance Imaging (MRI) is particularly adapted to these applications as the MRI efficiency (relaxivity) of a contrast agent can be made specifically responsive to a given physiological parameter. In contrast, in nuclear imaging such as PET (positron emission tomography) or SPECT (single photon emission computed tomography), the signal generated by the imaging agent is independent of its environment, while its intensity is directly related to probe concentration. Combining high sensitivity nuclear images with the excellent spatial resolution of morphological MRI in dual imaging has become common practice. Bimodal imaging is also attractive to access to quantitative detection of physiological parameters.[1, 2] Indeed, local concentration of the MRI probe should be known in order to unambiguously attribute observed variations in MRI signal to changes in relaxivity and not in probe concentration. Although this potential has been recognized early on, reports on bimodal agents for quantitative detection are scarce and limited to pH mapping.[3, 4] When metal ions or metabolites are concerned, additional requirements are needed: (1) the MRI responsive probe should be selective for the biomarker, adapted to its physiological concentration and (2) the nuclear probe should not perturb the MRI response. This last condition implies that the ratio radioactive element / cold parent element should be controlled and maximized.

The quantitative *in vivo* mapping of endogenous metal ions would be highly important as their spatial and temporal distribution is often not well known. Zn^{2+} is the second most important transition metal ion in the body, required for over 300 different cellular processes, including enzyme activities, DNA and protein synthesis or signaling. Brain, prostate, breast and pancreas have particularly high content in zinc (mM to µM depending on physiological or pathological state), in a range accessible by MRI.[5] Misregulation of zinc has been associated with cancers,[6] diabetes[7] and neurodegenerative diseases.[8] Nevertheless, its role is not completely understood[9] and remains an active area of research.[10, 11] There is a clear need for quantitative assessment of zinc by non-invasive imaging techniques.

Quantitative detection using small molecule bimodal agents can be achieved either by combining an MRI and a PET/SPECT reporter in the same molecule, or by injecting a cocktail of imaging agents for each technique. Both approaches have been applied to pH mapping,[3, 4] but cannot systematically be translated to cation detection. The advantage of the first method is a strictly identical biodistribution of the two reporters, but the sensitivity requirements for MRI and PET/SPECT are impossible to respect within a single molecule. Caravan et al. proposed to introduce a ^{18}F reporter on a pH sensitive contrast agent, which was diluted with ^{19}F to circumvent the sensitivity problem.[3] The tedious synthesis required to introduce the nuclear reporter is a major drawback of this method. In the second approach, a cocktail can be tuned to respect the sensitivity of each imaging technique, but one has to make sure that the biodistribution of the two molecules is similar. Aime et al. took advantage of the similar chemical properties of Ln^{3+} ions and used the mixture of a pH-responsive Gd^{3+} complex and its radioactive Ln^{3+} ($^{166}Ho^{3+}$) analogue.[4] With the production method used to obtain ^{166}Ho,

[a] Centre de Biophysique Moléculaire, CNRS UPR 4301, Université d'Orléans, Rue Charles Sadron, F-45071 Orléans 2, France. E-mail: celia.bonnet@cnrs.fr; eva.jakabtoth@cnrs.fr
[b] CEMHTI, CNRS UPR3079, Université d'Orléans, F-45071 Orléans 2, France.
[c] Université François Rabelais de Tours, Inserm, Imagerie et Cerveau UMR U930, Tours, France.
[d] Centre d'Imagerie du petit Animal, PHENOMIN-TAAM, CNRS UPS44, F-45071 Orléans 2, France.

Electronic Supplementary Information (ESI) available: synthetic procedures, potentiometric titrations, relaxometric and photophysical measurements, production, purification, radiolabeling, MRI images, and uncertainty calculations. See DOI: 10.1039/x0xx00000x

their sample was diluted in a high amount of ^{165}Ho. Although they managed to achieve pH detection, this approach would be unrealistic to detect biomarkers in µM or even mM concentration, as the high quantity of bulk ^{165}Ho present would strongly limit the attainable MRI response.

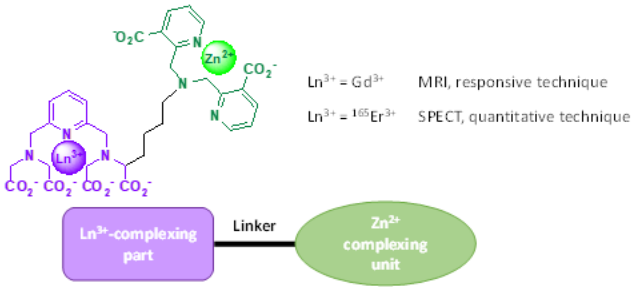

Fig. 1. Structure and schematic representation of the Zn^{2+}-responsive contrast agent.

Here, we propose to use $^{165}Er^{3+}$ and we demonstrate quantification of Zn^{2+} with a cocktail of the Zn^{2+}-responsive MRI agent GdL and its ^{165}ErL analogue. ^{165}Er has an optimal half-life ($t_{1/2}$ = 10.36 h vs 26.6h for ^{166}Ho),[12] and emits X-radiation (50 KeV), suitable for SPECT imaging.[13] It is readily produced from ^{165}Ho (stable isotope with 100 % abundance) in a cyclotron and can therefore be separated from the parent isotope because it is a different element. Thus the cocktail can be prepared without dilution of the MRI reporter (Gd^{3+} complex), contrary to the example above (see ESI).[4]

The ligand L consists of a polyaminocarboxylate unit with a pyridine backbone (Py) to chelate the Ln^{3+}, a linker, and a Zn^{2+} binding unit (Fig. 1). The relatively good thermodynamic stability and kinetical inertness of LnPy complexes ensure their safe use in animal studies, as previously demonstrated.[14] The Ln^{3+} has two inner sphere water molecules which are not replaced by physiological anions and confer high relaxivity to the Gd^{3+} complex.[15] The Zn^{2+} chelating moiety is a modified bis(pyridinylmethyl)amine (DPA) with an affinity for Zn^{2+} (K_d ca. 25 nM)[16] relevant for physiological applications.[5] We have introduced carboxylate functions on the DPA pyridines to potentially generate a change in the hydration number of the Gd^{3+} and to minimize the formation of dimers upon Zn^{2+} binding.[17]

Ligand L was synthesized in 6 steps. After the formation of the lanthanide complexing unit, a lysine derivative spacer and the Zn^{2+} complexing DPA unit were successively introduced. The full description is given in ESI.

Potentiometric titrations evidence the formation of a stable GdL complex, with log K_{GdL} = 20.1(1), more than one order of magnitude higher than that of the parent Py.[14] Mono- and bimetallic complexes are observed with Zn^{2+}, with affinity constants of log K_{ZnL} = 16.5(1) and log K_{Zn2L} = 9.9(1), respectively (see ESI for the full speciation). Log K_{GdL} is nearly four orders of magnitude higher than log K_{ZnL} demonstrating selectivity of the Py unit for Ln^{3+} over Zn^{2+}. The affinity of GdL for Zn^{2+} can be estimated from log K_{Zn2L}, and it is in the low nanomolar range, in accordance with Log $K_{ZnL'}$ = 9.08 of a model compound mimicking the Zn^{2+} binding site (unpublished results).

Upon addition of Zn^{2+} to a GdL solution, no significant relaxivity changes were observed (see ESI). This excludes variation in the hydration number of GdL. It was corroborated with luminescence lifetime measurements on the corresponding Eu^{3+} complexes, yielding two water molecules in the first coordination sphere of Gd^{3+} (q = 2.0(3), see ESI for details) in the absence or presence of Zn^{2+}. GdL contains three pyridine units which are known to interact with human serum albumin (HSA), and it was already demonstrated for DPA-containing agents that a relaxometric response to Zn^{2+} can be obtained in the presence of HSA.[18, 19] Indeed, the agent alone binds only weakly to HSA, whereas in the presence of Zn(II), the binding is stronger resulting in higher relaxivity. Here, in the presence of HSA, GdL shows a relaxivity increase of *ca.* 25 % upon Zn^{2+} binding (Fig. 2a). Importantly for quantitative detection, the relaxivity increases linearly with increasing amounts of Zn^{2+} (Fig. 2b). Both in the absence and in the presence of Zn^{2+}, the relaxivity is independent of GdL concentration (figure S3) implying that a relaxivity vs. [Zn^{2+}]/[GdL] calibration curve can be established (for a given temperature, magnetic field and HSA concentration). The selectivity of GdL for Zn^{2+} over other physiological cations has been assessed by relaxivity measurements (see ESI). GdL responds to Cu^{2+} as well, similarly

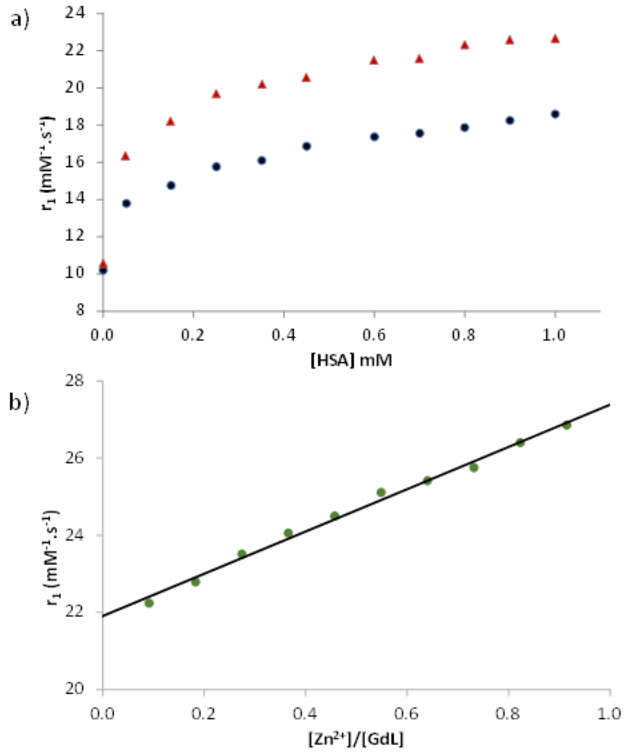

Fig. 2. ^{1}H relaxivity measurements at pH = 7.4 (Hepes 0.1 M), at 20 MHz, in the presence of [GdL] = 0.30 mM: a) as a function of HSA, in the absence (●), or in the presence of 1 eq. of Zn^{2+} (▲), at 310 K; b) in the presence of [HSA] = 0.6 mM, with increasing amounts of Zn^{2+} at 298 K.

to previously reported Zn^{2+}-responsive agents.[18, 20, 21] The *in vivo* concentration of Cu^{2+} in relevant tissues is at least one

order of magnitude lower than that of Zn^{2+}.‡ If such amount of Cu^{2+} is present next to Zn^{2+}, it induces less than 3 % variation of the relaxivity (see ESI), which is negligible with respect to the experimental uncertainty of the Zn^{2+} concentration determined (vide infra).

In order to achieve quantitative detection of Zn^{2+}, $^{165}Er^{3+}$ was produced, purified and its radionuclide purity was assessed by γ-spectrometry with a HPGe detector (Canberra). It was then reacted with L to yield ^{165}ErL. The complex was obtained quantitatively after 10 min at room temperature (see ESI for detailed ^{165}Er production, purification and ^{165}ErL preparation).

A cocktail with a known GdL/^{165}ErL mole ratio ($1/2.4x10^{-7}$), respecting the relative sensitivity of MRI and SPECT detection, was prepared in HSA solution (0.6 mM, physiological concentration). This solution was then diluted to give five samples, to which unknown concentrations of Zn^{2+} were added while keeping the HSA concentration constant at 0.6 mM for all samples. The activities were measured for all samples by γ-spectrometry. Then the samples were imaged using a γ-camera (Fig. 3b). The concentration of $^{165}Er^{3+}$ was calculated from the signal intensity, giving access to the Gd^{3+} concentration (by knowing the Gd/Er ratio). These Gd^{3+} concentrations correspond within 6 % to those calculated according to the dilutions and the concentration of the Gd^{3+} stock solution (which was determined by bulk magnetic susceptibility shifts (BMS)[22]). This is within the range of the experimental error (uncertainly) calculated to be *ca.* 16 % (see ESI). Finally, after total decay of the samples (*ca.* 1 to 2 weeks), a T_1-weighted MR image was recorded (Fig. 3a) on a 1.5 T scanner (Signa HDxt, General Electric, Milwaukee, USA). The longitudinal relaxation times measured were translated into relaxivity using the Gd^{3+} concentration calculated for each sample (see ESI). Based on a calibration curve recorded on the same MRI scanner and at the same temperature (Figure S6), the experimental Zn^{2+} concentrations were calculated from the measured relaxivities (Table 1). The experimental error on the Zn^{2+} concentrations was calculated to be 23% (see ESI). We also determined the Zn^{2+} concentration of each sample by ICP, and a very good agreement was obtained (the difference between the concentration measured by ICP and determined via relaxivity measurements is maximum 13 %, within the experimental error). For comparison, between healthy and malignant prostate tissue for instance, Zn^{2+} concentration varies from *ca.* 4 to 0.4 mM, representing a 90 % decrease in Zn^{2+} concentration.[5] To take full benefit of this quantitative method, we are developing more efficient systems for Zn^{2+} detection which maximize the relaxivity change upon Zn^{2+} complexation.

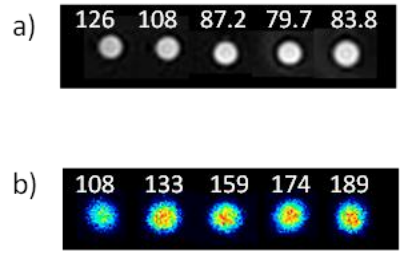

Fig. 3. T_1-weighted images of the five samples (T_1 values are given in ms) at 1.5 T using a spin echo sequence with TE = 9 ms, TR = 100 ms; T_1 were measured with variable TR from 20 to 2000 ms (a). Corresponding images from the γ-camera (activities are given in kBq) (b).

Table 1. Zn^{2+} concentration determined by the use of the bimodal cocktail of LnL (exp), and by ICP (th). Δ represents the difference between the two values. [Gd^{3+}] is calculated based on the activities of $^{165}Er^{3+}$ as described in the text.

	[Gd^{3+}] (mM)	[Zn^{2+}]$_{exp}$ (mM)	[Zn^{2+}]$_{th}$ (mM)	Δ (%)
Sample 1	0.30±0.05	0.33±0.08	0.32	3.0
Sample 2	0.37±0.06	0.29±0.07	0.29	0
Sample 3	0.44±0.07	0.54±0.13	0.49	9.3
Sample 4	0.49±0.08	0.62±0.14	0.55	11.3
Sample 5	0.53±0.09	0.10±0.03	0.094	6.0

To sum up, we report a proof-of-concept of quantitative assessment of Zn^{2+} concentration *via* combined MRI and SPECT detection using a Gd/$^{165}Er^{3+}$ cocktail. $^{165}Er^{3+}$ is easily produced and separated from ^{165}Ho and its half-life ($t_{½}$ = 10.36h) is adapted to medical imaging. The application of $^{165}Er^{3+}$ could be generalized to quantitative responsive imaging of other physiological cations, metabolites or any biomarker. Although the development of hybrid SPECT/MRI imagers is still in its infancy, a small number of systems are already under development, which could allow simultaneous detection by the two modalities.[23-25] Finally, given its accessibility in cyclotron facilities, $^{165}Er^{3+}$ is also an interesting surrogate to Gd^{3+} to perform *in vivo* biodistribution studies of potential MRI agents by SPECT.

We thank Agnès Pallier for performing ICP measurements on the samples. CSB thanks the support of the French National Research Agency (grant ANR-13-JS07-0007).

Conflicts of interest

There are no conflicts to declare.

Notes and references

‡ For example : synaptic cleft: 15 µM of Cu vs 300 µM of Zn [8]; prostate 7-50 nmol/g of Cu vs 3000-10000 nmol/g of Zn [26]; pancreas : 2 µg/g of Cu vs 88 µg/g of Zn for dogs [27].

1. R. T. M. de Rosales, *J. Labelled Compd. Radiopharm.*, 2014, **57**, 298-303.
2. L. Sandiford and R. T. M. de Rosales, *Pet Clinics*, 2016, **11**, 119-128.
3. L. Frullano, C. Catana, T. Benner, A. D. Sherry and P. Caravan, *Angew. Chem. Int. Ed.*, 2010, **49**, 2382-2384.
4. E. Gianolio, L. Maciocco, D. Imperio, G. B. Giovenzana, F. Simonelli, K. Abbas, G. Bisi and S. Aime, *Chem. Commun.*, 2011, **47**, 1539-1541.
5. L. De Leon-Rodriguez, A. J. M. Lubag and A. D. Sherry, *Inorg. Chim. Acta*, 2012, **393**, 12-23.
6. S. L. Kelleher, N. H. McCormick, V. Velasquez and V. Lopez, *Adv. Nutr.*, 2011, **2**, 101-111.
7. N. Wijesekara, F. Chimienti and M. B. Wheeler, *Diabetes Obesity & Metabolism*, 2009, **11**, 202-214.

8. P. Faller and C. Hureau, *Dalton Trans.*, 2009, DOI: 10.1039/b813398k, 1080-1094.
9. A. M. Banas and K. Banas, *J. Biol. Inorg. Chem.*, 2011, **16**, 9-13.
10. L. C. Costello and R. B. Franklin, *Expert Opin. Ther. Targets*, 2017, **21**, 51-66.
11. S. A. Myers, *Int. J. Endocrinol.*, 2015, **2015**, 167503-167503.
12. A. J. Amoroso, I. A. Fallis and S. J. A. Pope, *Coord. Chem. Rev.*, 2017, **340**, 198-219.
13. D. V. Rao, P. N. Goodwin and F. L. Khalil, *Journal of Nuclear Medicine*, 1974, **15**, 1008-1010.
14. C. S. Bonnet, F. Buron, F. Caille, C. M. Shade, B. Drahos, L. Pellegatti, J. Zhang, S. Villette, L. Helm, C. Pichon, F. Suzenet, S. Petoud and E. Toth, *Chem. Eur. J.*, 2012, **18**, 1419-1431.
15. L. Pellegatti, J. Zhang, B. Drahos, S. Villette, F. Suzenet, G. Guillaumet, S. Petoud and E. Toth, *Chem. Commun.*, 2008, 6591-6593.
16. J. K. Romary, J. D. Barger and J. E. Bunds, *Inorg. Chem.*, 1968, **7**, 1142-1145.
17. C. S. Bonnet, F. Caille, A. Pallier, J.-F. Morfin, S. Petoud, F. Suzenet and E. Toth, *Chem. Eur. J.*, 2014, **20**, 10959-10969.
18. A. C. Esqueda, J. A. Lopez, G. Andreu-De-Riquer, J. C. Alvarado-Monzon, J. Ratnakar, A. J. M. Lubag, A. D. Sherry and L. M. De Leon-Rodriguez, *J. Am. Chem. Soc.*, 2009, **131**, 11387-11391.
19. J. Yu, A. F. Martins, C. Preihs, V. Clavijo Jordan, S. Chirayil, P. Zhao, Y. Wu, K. Nasr, G. E. Kiefer and A. D. Sherry, *J. Am. Chem. Soc.*, 2015, **137**, 14173-14179.
20. J. L. Major, G. Parigi, C. Luchinat and T. J. Meade, *Proc. Natl. Acad. Sci. U. S. A.*, 2007, **104**, 13881-13886.
21. M. Regueiro-Figueroa, S. Guenduez, V. Patinec, N. K. Logothetis, D. Esteban-Gomez, R. Tripier, G. Angelovski and C. Platas-Iglesias, *Inorg. Chem.*, 2015, **54**, 10342-10350.
22. D. M. Corsi, C. Platas-Iglesias, H. van Bekkum and J. A. Peters, *Magn. Reson. Chem.*, 2001, **39**, 723-726.
23. P. Bouziotis and C. Fiorini, *Clin. Trans. Imaging*, 2014, **2**, 571-573.
24. M. J. Hamamura, S. Ha, W. W. Roeck, L. T. Muftuler, D. Jwagenaar, D. Meier, B. E. Patt and O. Nalcioglu, *Phys. Med. Biol.*, 2010, **55**, 1563-1575.
25. L. Cai, Z. M. Shen, J. C. Zhang, C. T. Chen and L. J. Meng, presented in part at the IEEE Nuclear Science Symposium conference record. Nuclear Science Symposium, Anaheim, USA, 27 October-03 November 2012, 2012.
26. D. Denoyer, S. A. S. Clatworthy, S. Masaldan, P. M. Meggyesy and M. A. Cater, *The Prostate*, 2015, **75**, 1510-1517.
27. K. Adamama-Moraitou, T. Rallis, A. Papasteriadis, N. Roubies and H. Kaldrimidou, *Dig. Dis. Sci.*, 2001, **46**, 1444-1457.